# Accurate Determination of the $\mu^+$ Magnetic Moment*

R. L. GARWIN,† D. P. HUTCHINSON, S. PENMAN,‡ AND G. SHAPIRO§
*Columbia University, New York, New York*

(Received August 4, 1959)

Using a precession technique, the magnetic moment of the positive mu meson is determined to an accuracy of 0.007%. Muons are brought to rest in a bromoform target situated in a homogeneous magnetic field, oriented at right angles to the initial muon spin direction. The precession of the spin about the field direction, together with the asymmetric decay of the muon, produces a periodic time variation in the probability distribution of electrons emitted in a fixed laboratory direction. The period of this variation is compared with that of a reference oscillator by means of phase measurements of the "beat note" between the two. The magnetic field at which the precession and reference frequencies coincide is measured with reference to a proton nuclear magnetic resonance magnetometer. The ratio of the muon precession frequency to that of the proton in the same magnetic field is thus determined to be $3.1834\pm0.0002$. Using a re-evaluated lower limit to the muon mass, this is shown to yield a lower limit on the muon $g$ factor of $2(1.00122\pm0.00008)$, in agreement with the predictions of quantum electrodynamics.

## I. INTRODUCTION

RECENT developments in the theory of weak interactions[1] make it appear that many of the properties of the mu meson can be accounted for on the assumption that it enters into interactions in the same way as the electron but has a much larger mass. The electromagnetic properties of the muon, therefore, acquire increased interest as a further test of the identity of the interactions of the two particles.

Quantum electrodynamics[2] makes the prediction that the magnetic moment of a spin $\frac{1}{2}$ Dirac particle is 1.00116[3] times that predicted by Dirac theory, $e\hbar/mc$. The anomalous magnetic moment of the electron does indeed agree with this prediction.[4] Application of similar calculations to the muon involves the extension of electrodynamics into a more relativistic region than required in the case of the electron. For instance, existence of a finite cutoff to the theory would result in a magnetic moment closer to the Dirac prediction.[5]

The present experiment is a measurement of the magnetic moment of the mu meson. Comparison of the result with theory depends on accurate knowledge of the muon mass. In Sec. VI, the experimental determination of the lower limit to the muon mass is discussed, and a corresponding lower limit to the $g$ factor is derived.

The existence of polarized muon beams and a means of detecting the direction of polarization via their asymmetric decay[6] made possible the measurement of the muon magnetic moment. In the original experiment it was found necessary, to obtain agreement with the asymmetry curve, to assume a value of the moment close to the Dirac prediction. In this way the value was determined to an accuracy of 1%. The Liverpool group,[7] using an analog time-to-height converter to record the distribution in time of the emitted electrons, achieved an accuracy of 0.7%. A resonance technique, in which the muons were stopped in a large static magnetic field oriented parallel (or antiparallel) to the direction of initial polarization, and were then re-oriented by an rf oscillating field perpendicular to it, was employed at this laboratory.[8] The reversal in polarization was detected by a change in the counting rate of electrons emitted along the initial muon spin direction. The result of that experiment for the ratio of the muon moment to that of the proton is $3.1865\pm0.0022$.

The finite lifetime of the muon introduces a width into any frequency determination given by $\Delta\omega\Delta t\approx1$. Higher accuracy, therefore, necessitates going to higher fields and higher frequencies. The resonance technique suffers from the difficulty of producing rf fields of sufficiently high intensity. The precession method, making more sophisticated use of the electron time distribution was, therefore, employed. The Chicago group[9] formed coincidences between the emitted electron and the negative half of a 48.63 Mc/sec oscillator triggered by the stopping muon. They report $f_\mu/f_p=3.1838\pm0.0008$.[10]

In the present case, a precession technique is again employed. Muons brought to rest in a bromoform

* Supported by the joint program of the Office of Naval Research and the U. S. Atomic Energy Commission.

† Also at the International Business Machines Watson Laboratory, Columbia University.

‡ Now at the University of Chicago, Chicago, Illinois.

§ John Tyndall Fellow.

[1] M. Gell-Mann, Gatlinburg Conference on Weak Interactions, Revs. Modern Phys. (to be published).

[2] See, for example, W. Heitler, *The Quantum Theory of Radiation* (Oxford University Press, New York, 1954), 3rd ed., p. 311 ff.

[3] E. R. Cohen and J. W. DuMond, Phys. Rev. Letters **1**, 291 (1958).

[4] S. Koenig, A. Prodell, and P. Kusch, Phys. Rev. **88**, 191 (1952).

[5] V. B. Berestetskii, O. N. Krokhin, and A. K. Khlebnikov, J. Exptl. Theoret. Phys. (U.S.S.R.) **30**, 788 (1956) [translation: Soviet Phys. JETP **3**, 761 (1956)].

[6] R. L. Garwin, L. M. Lederman, and M. Weinrich, Phys. Rev. **105**, 1415 (1957).

[7] J. M. Cassels, T. W. O'Keefe, M. Rigby, J. R. Wormald, and A. M. Wetherell, Proc. Phys. Soc. (London) **A70**, 451 (1957).

[8] C. T. Coffin, R. L. Garwin, S. Penman, L. M. Lederman, and A. M. Sachs, Phys. Rev. **109**, 973 (1958).

[9] R. A. Lundy, J. C. Sens, R. A. Swanson, V. L. Telegdi, and D. D. Yovanovitch, Phys. Rev. Letters **1**, 38 (1958).

[10] R. A. Lundy, J. C. Sens, R. A. Swanson, V. L. Telegdi, and D. D. Yovanovitch (private communication).

target situated entirely within a very uniform magnetic field at right angles to the spin, will precess about the field direction with the Larmor frequency, $geH/2mc$. The time distribution of electrons emitted in a given direction is the product of the exponential decay of the muon and the rapid sinusoidal variation as the muon spin rotates. To record this distribution directly would tax the capacity of any pulse-height-analyzer's memory, and place severe requirements on the linearity of the time-to-pulse height converter. Therefore, the total elapsed time between the stopping of the muon and the detection of the decay positron was not recorded, but only the difference between this time and the nearest integral number of cycles of a fixed reference oscillator. Positrons for which the elapsed time after mu stopping differed by a whole number of cycles were stored as counts in the same channel of the pulse-height analyzer. Thus, the display observed was the superposition of many cycles of precession. If the reference oscillator frequency is the same as the precession frequency, the contributions from each of the cycles reinforce each other; and the folded distribution is one cycle of the $(1+a\cos\theta)$ periodic distribution. If the two frequencies are far different, the contributions from the various cycles will interfere destructively, and the folded distribution is flat. If the two frequencies are only slightly different (that is, their difference is less than the reciprocal lifetime of the muon), the folded distribution will still display the cosine term, but it will be reduced in amplitude, and in general shifted in its phase. These changes are a function of the difference between the two frequencies, the length of the gate during which electrons are accepted, and the delay between the time of the stopping of the muon and the opening of this gate. In particular, as is shown in Sec. II, the phase shift is a sensitive function of this delay and the frequency difference.

In this experiment two electron gates with different initial delays are employed, yielding folded distributions which are stored separately. The difference in phase between these distributions is then used as a measure of the departure from "resonance" (at which the two phases should be the same).

## II. MATHEMATICAL DESCRIPTION

The probability that an electron will be detected in a counter telescope subtending a solid angle $d\Omega$, during a time interval $dt$, occurring at an elapsed time $t$ after the muon came to rest, is

$$N_t dt = e^{-t/\tau}[1+a\cos(\omega_H t-\theta)](d\Omega/4\pi)(dt/\tau), \quad (1)$$

where $\tau$ is the muon mean life; $\omega_H$ is its precession frequency in a magnetic field $H$; $\theta$ is the angle between the direction of the initial muon spin and the momentum of the electron; $a$ is the product of the decay asymmetry parameter, beam polarization, and depolarization factor of the target material.

$$\text{Let } \Phi=\omega_0 t,$$

where $\omega_0$ is the frequency of the fixed reference oscillator.

$$\text{Further, let } \Phi=\phi+2\pi n,$$

where $n$ is an integer such that $0\leq\phi\leq 2\pi$. Then

$$N_\Phi d\Phi = e^{-\Phi/\omega_0\tau}\left[1+a\cos\left(\frac{\omega_H}{\omega_0}\Phi-\theta\right)\right]\frac{d\Phi}{\omega_0\tau}\frac{d\Omega}{4\pi}, \quad (1a)$$

and

$$N_\phi=\sum_{n=0}^{\infty} N_\Phi(\phi+2\pi n) \quad (2)$$

Thus, $N_\phi$ is exactly what is displayed on the pulse-height analyzer as a result of the folding process, modulo the period of the reference oscillator. It now remains to analyze the distribution so as to derive the magnetic moment as accurately as possible. The summation (2) is easily performed, using $\cos u=\mathrm{Re}(e^{iu})$, as a geometric series, with the result

$$N_\phi d\phi=\left[1+\frac{1}{R}a\cos\left(\frac{\omega_H}{\omega_0}\phi-\theta-\alpha_0\right)\right]\times e^{-\phi/\omega_0\tau}\frac{d\phi}{2\pi}\frac{d\Omega}{4\pi}f(\omega_0), \quad (3)$$

where

$$f(\omega_0)=2\pi(\omega_0\tau)^{-1}(1-e^{-2\pi/\omega_0\tau})^{-1}=1+\pi/\omega_0\tau-\cdots.$$

The salient features of this distribution are the amplitude reduction factor, $R$, and the phase shift, $\alpha_0$. These are functions of the difference between precession and reference frequencies, given by

$$Re^{i\alpha_0}=\frac{1-\exp(-2\pi/\omega_0\tau)}{1-\exp[-2\pi/\omega_0\tau+2\pi i(\omega_H-\omega_0)/\omega_0]}. \quad (4)$$

For $|\omega_H-\omega_0|\ll\omega_0$, which is always the case in this experiment, the approximate formulas hold that

$$R=[1+(\omega_H-\omega_0)^2\tau^2]^{\frac{1}{2}}, \quad (5a)$$

$$\tan\alpha_0=(\omega_0-\omega_H)\tau. \quad (5b)$$

These quantities may be recovered from a given experimental $N_\phi$ by a Fourier analysis (which in this case is equivalent to a least-squares fitting of the parameters $R$ and $\alpha_0$). Several alternative ways of using such data suggest themselves: (1) The function $R^{-1}$ may be plotted *vs* magnetic field; it will have its maximum point when the two frequencies are the same. Equation (5a) shows that this peak will not be sharp (see Fig. 6), and the statistics required to obtain a result with the desired degree of precision (0.01%) make this method impractical. (2) The function $\alpha_0$, which is much more sensitive to small frequency

differences, may be plotted *vs* magnetic field, passing through zero at "resonance." However, precise knowledge of $\alpha_0$ requires knowledge of the geometric angle $\theta$ to the same precision, as well as of the phase shifts introduced by time delays throughout the electronic measuring apparatus (and the assurance that the latter do not change during the course of the data-taking). Such knowledge and such assurance are not generally available. (3) The Chicago technique[9] corresponds to observing just the number of counts in that channel of the PHA display for which $(\phi-\theta)=0$. This number is then proportional to $[1+(a/R)\cos\alpha_0]$, provided the setting is correct and does not drift.

In the present experiment systematic difficulties due to uncertainties in the geometric and electronic phase shifts are avoided by comparing two sets of data collected during the same run. It will be shown that such shifts and drifts are cancelled out by this procedure, *provided they are the same for both sets.*

### Effect of Delaying the Electron Gate

If electrons are not accepted until after $t=T$, the sum in (2) must be taken from $n=\omega_0 T$ to infinity. The result is

$$N_\phi(\text{delay}=T)=e^{-T/\tau}\{1+(a/R)\cos[(\omega_H/\omega_0)\phi-\theta-\alpha_0+(\omega_H-\omega_0)T]\}e^{-\phi/\omega_0\tau}(f/2\pi)(d\Omega/4\pi), \quad (6)$$

which is the same as (3) except for the factor $\exp(-T/\tau)$, to account for the fact that some of the muons have disappeared before the gate is opened, and the additional phase term, $(\omega_H-\omega_0)T$, which expresses the fact that the "initial" spin direction (by which is meant the direction of the muon spin at the time when $\phi=0$ during the first cycle after the gate is opened) has been changed due to the precession.

### Effect of Finite Gate Length

If electrons are accepted only from $t=T$ until $t=T+G$, the distribution becomes

$$N_\phi\ (\text{delay } T,\ \text{gate } G)=N_\phi\ (\text{delay}=T)-N_\phi\ (\text{delay}=T+G),$$

$$N_\phi=(e^{-T/\tau}-e^{-(T+G)/\tau})\left[1+\frac{a}{RR_G}\cos\left(\frac{\omega_H}{\omega_0}\phi-\alpha\right)\right]\times e^{-\phi/\omega_0\tau}\frac{f}{2\pi}\frac{d\Omega}{4\pi}, \quad (7)$$

where

$$\alpha=\alpha_0+\theta-(\omega_H-\omega_0)T+\alpha(G), \quad (8)$$

and

$$R_G e^{i\alpha(G)}=\frac{1-\exp(-G/\tau)}{1-\exp[-G/\tau+i(\omega_H-\omega_0)G]}. \quad (8a)$$

$R_G$ oscillates, as a function of $\omega_H$, between 1 and $\tanh(G/2\tau)$, the oscillations becoming smaller and faster as $G$ increases.

$$\tan\alpha(G)=\frac{\sin(\omega_H-\omega_0)G}{\exp(+G/\tau)-\cos(\omega_H-\omega_0)G}. \quad (9)$$

This additional phase shift may be interpreted as being due to the change in the position of the centroid of the time distribution when the gate length is shortened. This may be seen as follows. For $|(\omega_H-\omega_0)G|\ll 1$

$$\alpha(G)\approx(\omega_H-\omega_0)\frac{Ge^{-G/\tau}}{1-e^{-G/\tau}}=(\omega_H-\omega_0)\Delta\bar{t}, \quad (10)$$

where

$$\Delta\bar{t}=\frac{\int_0^\infty te^{-t/\tau}dt}{\int_0^\infty e^{-t/\tau}dt}-\frac{\int_0^G te^{-t/\tau}dt}{\int_0^G e^{-t/\tau}dt}. \quad (11)$$

In this experiment, separate measurements were made of the $\phi$ distribution of electrons falling within two different gates: the first from $t=0$ until $t=T_1$ (the "early" gate); the second from $t=T_1$ until $t=T_2$ (the "late" gate). The quantity $\alpha$ of Eqs. (7) and (8) is determined (to within an arbitrary constant) for each, by Fourier analysis. Then, with no approximation,

$$\alpha_{\text{early}}-\alpha_{\text{late}}=(\omega_H-\omega_0)T_1-\alpha(T_2)+\alpha(T_1), \quad (12)$$

where $\alpha(T_1)$ and $\alpha(T_2)$ are given by Eq. (9). For $T_1=T_2$, the graph of early-late phase shift *vs* magnetic field is a straight line, passing through zero when $\omega_H$ and $\omega_0$ are the same. If the gate lengths are different this graph still has the same intercept, and is an antisymmetric function of the frequency difference, independent of what these frequencies are. For the usual choices of gate length, the curve is quite linear over the range of interest. For example if, as in this experiment, $T_1=1.75$ microseconds, $T_2=3.9$ microseconds, the curve can be approximated by a straight line of slope 0.855 degree/kilocycle, to within 0.1 degree out to 50 kc/sec, and to within 0.5 degree out to 100 kc/sec. In practice the experimental points are fitted to a straight line by least squares, and the slope is seen to agree with the prediction.

The above gives an estimate of the ultimate sensitivity of this technique. If a phase angle can be measured to within five degrees, which is readily done with the present apparatus, then the frequency may be determined to within 6 kc/sec. Greater precision is obtained by working at higher frequencies, limited eventually by the time resolution of the system (which must be better than $\frac{1}{3}$ the period of the oscillator) and the homogeneity of the magnetic field.

## III. SYSTEM DESCRIPTION

A particle stopping in the target is indicated by the coincidence $123\bar{4}$ (see Fig. 1 for arrangement of counters), and a decay electron in the forward or back-

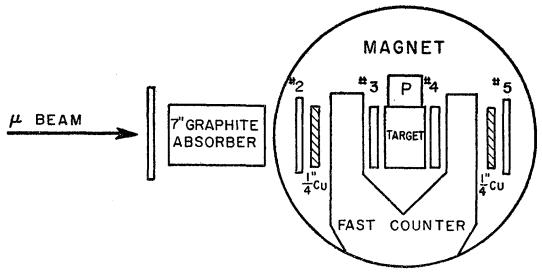


FIG. 1. Experimental arrangement. $P$=nuclear magnetic resonance probe. Muons coming to rest are identified by a $123\bar{4}$ coincidence. The decay electron gives a $45\bar{1}\bar{3}$ (forward electron) or $23\bar{1}\bar{4}$ coincidence falling within a 5.7 μsec gate.

ward direction is indicated by a coincidence $45\bar{1}\bar{3}$ or $23\bar{1}\bar{4}$, respectively, falling within a 5.7-microsecond gate triggered by the $123\bar{4}$ coincidence. The gate has an initial delay of 0.15 microsecond to insure that muons and prompt electrons will not be confused with each other. Both forward and backward electrons are processed by the same circuits, but the information is routed to different groups of channels of a commercial pulse-height analyzer (manufactured by PENCO, Model No. PA-4) by an external addressing circuit. The latter circuit also discriminates between electrons appearing before and after a variable delay time, $T_1$, storing them separately. A given event is thus stored in one of four groups of channels corresponding to late-front, early-front, late-back, or early-back.

Figure 2 gives a block diagram showing the relation between the various electronic circuits.

For the timing of the events, an additional counter, labeled Fast Counter, is employed. This counter has a forked light pipe with two $\frac{3}{8}$-in. thick plastic scintillators attached, one on either side of the target so that the stopping mu mesons and the electrons emitted in the forward and backward directions are all timed using the same phototube. Thus any long-term drift in the characteristics of the tube affect all the timing pulses the same. The output of this 6810A photomultiplier is overclipped with a shorted cable, and the time at which the originally negative pulse is just cancelled by its own reflection and becomes positive is taken as the timing criterion for the pulse involved. This minimizes timing jitter caused by fluctuating pulse height.[11] The positive portion of the output is amplified by a distributed stage employing EFP-60 tubes set on the edge of conduction. This "zero-crossing detector" gives saturated output pulses for positive inputs of about 0.5 v; the inputs employed in the actual run had positive portions of about 10 v. The time jitter due to finite rise time coupled with varying amplitude was thus minimized. The final stages of this amplifier are separated into two branches. Each one is gated by a 0.2 μsec pulse triggered for one branch by the μ stopping and for the other by a gated electron.

The output of the zero-crossing detector is used to trigger one of the pulsed oscillators, which then oscillates for 6 μsec at a frequency either one Mc/sec higher or lower than that of the reference oscillator (at a given time both pulsed oscillators have the same frequency, but this may be changed for both of them together

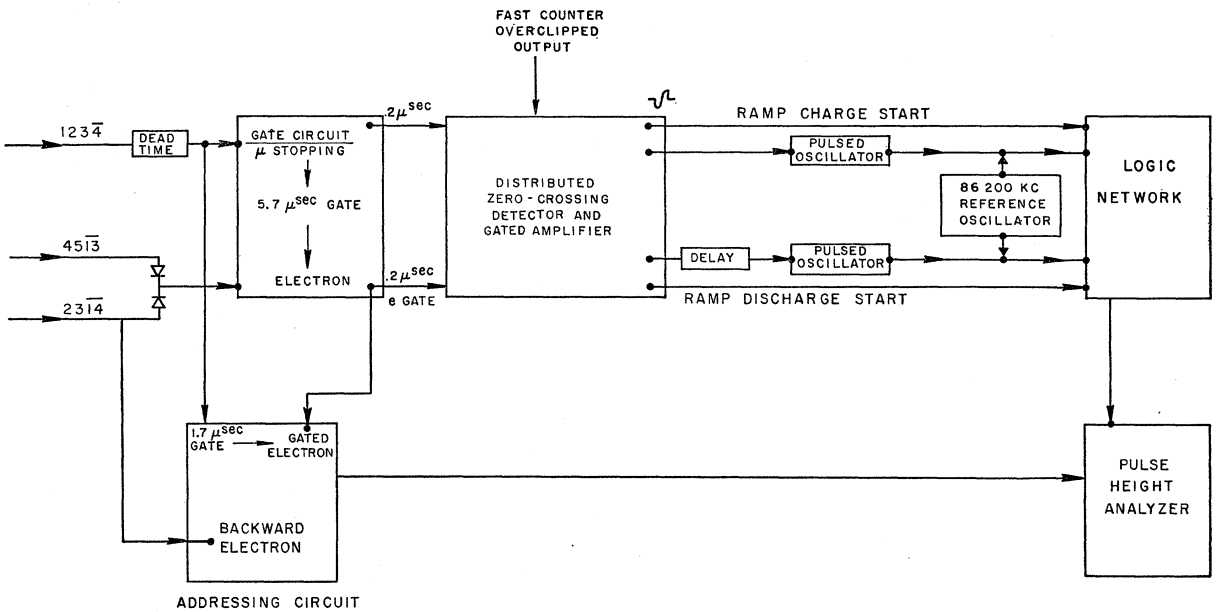


FIG. 2. Block diagram of electronics. The fast counter output, when gated by the appropriate identifying coincidence, initiates the triggering of the proper pulsed oscillator. The latter signal is mixed with the reference oscillator, and the beat note analyzed by the logic network. The output is routed to the proper group of channels in the pulse-height analyzer, by means of the addressing circuit.

[11] H. W. Lefevre and J. T. Russell, Rev. Sci. Instr. **30**, 159 (1959).

during the course of the experiment). The pulsed oscillator output is mixed with that of the continuously running reference oscillator, whose frequency for this experiment is 86.200 Mc/sec. The mixed signal is fed into the "logic" circuit (so-called because of the many logical operations it performs) which uses the detected envelope of the mixed frequencies. The idea of expanding the time scale by beating rung oscillators having slightly different frequencies has been used by Cottini and Gatti.[12] A related type of time vernier was used by Lefevre and Russell.[11] Our apparatus has more in common with that of Chase and Higinbotham.[13]

The envelope of the mixed signal is a 1 Mc/sec periodic waveform whose phase is determined by the phase of the reference oscillator at the instant the pulsed oscillator was started, and by the (fixed) starting phase of the pulsed oscillator. Subtracting the measured phase for the electron timing pulse from that for the corresponding $\mu$ stopping yields the quantity $\phi$ defined in Sec. II.

Figure 3 shows the timing sequence of the processes in the logic circuit. An output pulse from the zero-crossing detector is used to start a condenser charging (or discharging) at a constant rate. The mixed reference-oscillator-pulsed-oscillator wave is demodulated, converted to a square wave, and then differentiated to form a series of alternating polarity pulses, each one corresponding to a zero-crossing of the "beat note." The condenser charging (or discharging) stops at the first such positive-going zero-crossing which follows a set time delay, sufficient to allow starting transients to disappear. The voltage remaining on the condenser after both the $\mu$ and $e$ channels have completed their cycle of operation is then read out, and a count is stored in the pulse-height analyzer in one of the group of channels actuated by the addressing circuit. Delays are arranged so that the discharging of the condenser (actuated by the electron) does not begin until the charging (actuated by the muon) is complete.

Note that since both $\phi_\mu$ and $\phi_e$ can fall between 0 and $2\pi$, their difference can fall anywhere between $-2\pi$ and $+2\pi$. Thus if a single pulse is made to simulate both electron and mu, and the pulse-height analyzer is operated normally, without external addressing, all the counts (assuming perfect resolution) will be stored in two single channels, spaced a distance corresponding to $2\pi$ radians apart. That this is so is easily seen once it is realized that, although $(\Phi_e-\Phi_\mu)$ is now the same for all counts, $\phi_e$ is randomly distributed, and in a certain fraction of the cases will be smaller than $\phi_\mu$. In that case the counts will be stored in a channel corresponding to $\phi-2\pi$. Throwing a small delay into either branch will displace both these channels by the same amount, changing the distribution of counts between them. The gain setting may then be adjusted so that the separation is exactly ten channels.

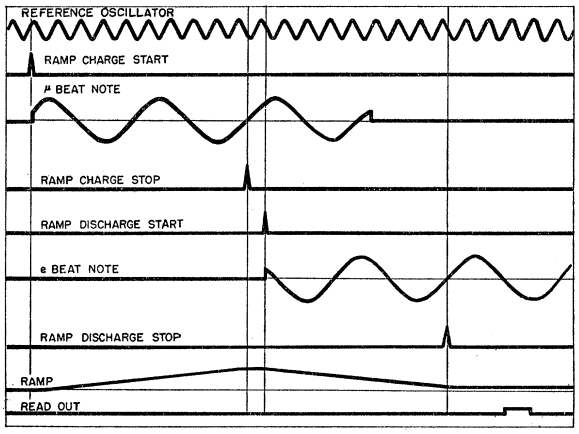


FIG. 3. Timing diagram of logic network (not to scale). Beat notes have phase equal to that of the reference oscillator at time of respective Ramp Start. Ramp Stops occur at a positive-going zero-crossing after a delay to avoid transients.

When the pulse-height analyzer is addressed externally in the present system, the "tens" addressing is interrupted so that counts which would ordinarily be stored in channels 11, 21, 31, etc., are all stored in channel 1. The tens address is then supplied by the external addresser, depending on the nature of the event. Thus late-front events are stored in channels 10–19, early-front in channels 30–39, etc. The folded displays obtained have the effect of removing the above-mentioned ambiguity of $2\pi$, since in all cases counts corresponding to the same $\phi$ will be stored in the same units channel.

Thus at the end of each run one has four distributions, $N_\phi$. The forward and backward electrons are treated separately; they serve to increase the statistics for a given running time, but are otherwise unrelated to each other for our purposes. For each group the quantity $\alpha$ is calculated.

$$\alpha=\arctan\sum_{i=1}^{10}N_i\sin\phi_i\Big/\sum_{i=1}^{10}N_i\cos\phi_i, \qquad (13)$$

where $N_i$ is the number of counts stored in the channel whose phase angle is $\phi_i$. This is equivalent to a least square fit with phase angle as a parameter. The numerator is proportional to the coefficient of the $\sin\phi$ term in the Fourier analysis of $N_\phi$. The denominator is proportional to the coefficient of $\cos\phi$. The standard deviation of $\alpha$ is given by

$$(\Delta\alpha)^2=\sum_i\left(\frac{\partial\alpha}{\partial N_i}\right)^2 N_i = \frac{\frac{1}{2}\sum_i N_i}{(\sum_i N_i\sin\phi_i)^2+(\sum_i N_i\cos\phi_i)^2}. \qquad (14)$$

Averages of $\alpha_{\text{early}}$-$\alpha_{\text{late}}$ are formed for forward and back-

[12] C. Cottini and E. Gatti, Nuovo cimento 4, 1550 (1956).
[13] R. L. Chase and W. A. Higinbotham, Rev. Sci. Instr. 28, 448 (1957).

ward electrons and over the several runs at the same magnetic field. The plot of early-late phase shift *vs* magnetic field follows Eq. (12). This phase shift passes through zero when $\omega_H=\omega_0$. Thus if the measured $(\alpha_{\text{early}}-\alpha_{\text{late}})$ is plotted *vs* $H$ the intercept $\alpha=0$ gives $H$ for $\omega_0=\omega_H$.

It should be noted that use may be made of Eq. (12) directly. From measurements made at a *single* setting of the magnetic field, the distance from resonance may be calculated. This relation is useful especially in the early stages of the experiment when the resonance is being sought. It suffers from the small disadvantage that the gate times must be measured accurately.

## IV. OTHER EQUIPMENT

### A. Magnet

The pole faces of the magnet are $3\frac{5}{16}$ in. apart and 11 in. in diameter, made of Armco iron. There are circular rings 9-in. inside diameter by 11-in. outside diameter, $\frac{1}{4}$ in. thick, at the perimeters. Fine shimming is accomplished with rings of one and two-mil shim stock cemented to the pole faces. At a field of 6357 gauss, the uniformity of the field over a volume 2 in. high by 3 in. long by 1 in. thick in the center of the field, is such that the root-mean-square deviation from the average is 40 parts per million. The field was mapped several times before, during and after the run; and the volume averages of the field calculated in each case (relative to the field at the center of the gap) do not deviate from each other by more than 10 ppm.

In the mapping of the field, and in the subsequent monitoring, a nuclear magnetic resonance probe is fastened to a rigid arm which is mounted on a milling machine bed. The center of the probe in the monitor position is midway between the pole faces $1\frac{7}{8}$ in. from the axis. The difference between the field at this position and that in the center of the gap is reproducible to within 30 ppm of the total field.

### B. Target

The target used was bromoform in a copper container measuring 2 in.$\times 2\frac{1}{2}$ in.$\times\frac{7}{8}$ in. overall. The walls were of such thickness that the copper did not occupy more than 20% of the total volume. A stand was provided so that the target could be positioned reproducibly in the most uniform part of the field.

### C. Regulator

The transistor current regulator used with the magnet is described elsewhere.[14] The proton magnetic resonance is displayed on an oscilloscope and continuously monitored. The proton oscillator is continually calibrated by zero-beating with a crystal-calibrated frequency meter (U. S. Navy type CKB 74028). A shift of 40 ppm would be easily visible and can be corrected manually by adjusting the potentiometer controlling the error signal for the regulator. It is estimated that the regulation is such that the time average of the magnetic field during a run does not differ from its nominal value by more than a least count of the frequency meter, or 15 ppm.

### D. Reference Oscillator

The reference frequency is provided by a General Radio signal generator oscillating at a fundamental frequency of 28.733 Mc/sec. A frequency tripler circuit generates the third harmonic, and this signal is then fed through two isolating amplifiers (Hewlett-Packard distributed type B) before being mixed with the pulsed oscillator outputs. The frequency of this signal is checked repeatedly with a frequency meter. Both this meter and the one used to calibrate the nuclear magnetic resonance are themselves calibrated against the nearest 10-kc/sec subharmonic of the same 1-Mc/sec crystal oscillator. Thus, even if this crystal is not exactly 1 Mc/sec, the ratio $f_\mu/f_p$ will be given correctly. The linear scales of the frequency meters are relied upon only to interpolate between the 10-kc/sec harmonics.

### E. Counters

The accurate timing in this experiment is made possible by the large current handling capabilities, as well as by the low transit time spread of the 6810A photomultiplier tube. The use of these tubes is facilitated by a cathode follower string described elsewhere.[15]

The remaining counters, except for counter No. 1, are limited in size by the necessity of fitting inside the magnet. They are all $\frac{3}{16}$ in. thick, $2\frac{3}{4}$ in. high, and 3 in. to 4 in. long, except counter No. 3, which is cut so as just to cover the target, in order to minimize background. Sufficient carbon absorber is placed in between counters No. 1 and No. 2 to stop all pions, and leave the muons with just enough range to stop in the bromoform target.

Two copper plates, each $\frac{1}{4}$ in. thick, are inserted between the fast counter and counters No. 2 and No. 5, respectively, to stop the low-energy emitted positrons, and hence enhance the asymmetry.

## V. CHECKS ON SYSTEMATICS

The systematic requirements on the performance of the equipment are severe. There are two general categories:

(a) The system must be aperiodic; i.e., no spurious "asymmetries" or "effects" must be introduced which would confuse the interpretation of the data, or so distort them as to lead to an incorrect result.

(b) The system must be uniform; i.e., all events must be treated identically, and in particular there

[14] R. L. Garwin, D. P. Hutchinson, S. Penman, and G. Shapiro, Rev. Sci. Instr. **30**, 105 (1959).

[15] S. Penman, Rev. Sci. Instr. (to be published).

must be no difference in the processing of "early" and "late" events in all stages of the equipment, within very narrow tolerance.

An upper limit on the existence of aperiodic effects can be placed by making certain changes in the setup, and requiring that the system behave in a prescribed manner. Thus the effects observed are demonstrated to be real. Of the residual, undetected asymmetries of the system, their effect can be reduced, if not completely cancelled, by averaging the data over various situations in which equipment aperiodicity would have mutually opposite effects.

The seriousness of nonuniformity can be recognized from the fact that a systematic shift of five degrees over 100 cycles (that is, a timing shift of 0.1 nanosecond over a period of 1 $\mu$sec) will produce an error of 0.01% in the results. Since there are no standards readily available to produce a time interval of that duration to that accuracy, the problem of testing for such shifts was raised. Preliminary reports of this experiment contain erroneous results because such an error was undetected.

### A. Recovery of Zero-Crossing Detector

Both the muon and the electron timing pulse are amplified by the same distributed stage of the zero-crossing detector, within a few microseconds of each other. If the circuit has a recovery time of this order of magnitude, this will give rise to a systematic delay in the second of the two (the electron pulse) which depends on how soon it follows the first. Such a dependence was actually shown to exist in the original circuit by the following test. An artificial pulse was used to simulate a muon, and the same pulse, delayed by a few microseconds was used to simulate an electron. The PHA display was that of two single-channel peaks separated by $2\pi$, as explained previously. The same pulse was then used a third time, intermediate between the simulated muon and electron, to fire the distributed stage; so that the state of recovery of the circuit, at the time of the simulated electron, was altered. A shift as large as 1/20 of a cycle was observed in the resulting display. Such a shift, occurring over a period of 100 cycles, is capable of introducing a systematic error of 0.05%.

This source of error was remedied by *increasing* the recovery time of the circuit. For it will be seen that if the recovery time is 50 $\mu$sec, the variations in characteristics over a 6 $\mu$sec gate will be small, and all electron timing pulses will be delayed by the same amount. The freedom of the system from systematic errors of this nature was then demonstrated in the following fashion.

An artificial source of correlated pulses was formed by modulating the grid of a phototube with the thirty-volt output of a second signal generator operated at or near the reference frequency. Pulses were produced by exposing the counter to random radiation from a beta source. There was almost complete correlation in time between pulses accepted above a given threshold, and the modulating signal. One of these pulses was selected at random as the simulated muon, and the pulse next following it as the simulated electron. Thus a correlation between these two was achieved, analogous to that between a precessing muon and its decay electron. The full apparatus was then run in a simulated experiment.

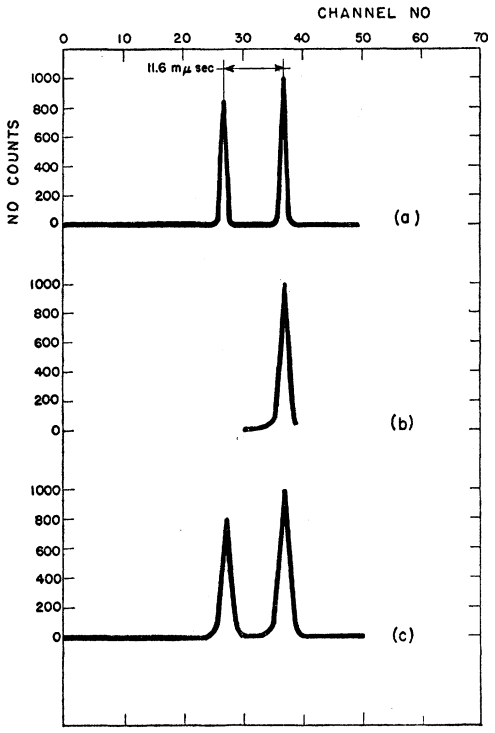


FIG. 4. Time resolution of the system. (a) The same input is used to trigger both pulsed oscillators. (b) Same as (a) folded into ten channels. (c) Coherent inputs from two phototubes focused on the same scintillator.

When the modulating signal was set at exactly the reference frequency, no early-late phase shift was detected, to within an uncertainty of 0.001%. When the frequency was varied the expected phase shifts were observed.

### B. Time Resolution

The time resolution of the entire system can be tested rigorously by feeding pulses with a fixed time separation into both branches. The counts fall into two channels separated by one cycle (of 86.2 Mc/sec) corresponding to 11.6 nanoseconds. The separation is set at 10 channels. Figure 4(a) shows the actual distribution obtained when the same pulse simulates mu and electron. The resolution is clearly better than one channel, or 1.2 nanoseconds. Figure 4(b) shows a similar distribution with the PHA addressed externally so that the 20-channel distribution in 4(a) is folded into

10 channels, and the two peaks are superimposed. Figure 4(c) shows the 20-channel distribution when the simulated mu and electron are not the same pulse, but are the outputs of two different photomultipliers viewing the same scintillator, which is exposed to a beta source. The optical coupling was poor so that the pulse sizes are much smaller and the statistical fluctuations larger than would be expected during the experiment. The time resolution is, nevertheless, quite good—better than 1 nanosecond half-width at half maximum.

The time resolution is checked by this method before and after each one-hour run. If the channel in which the peaks fall had changed, or the separation had become different from 10 channels, or the peaks become broader, the proper adjustments are made to restore the system to its original conditions (by adjusting gains of amplifiers, frequencies of pulsed oscillators, or charging rate of condenser). In no case was this change greater than half a channel. Since both early and late events are affected alike, the consequence of a drift is only to broaden the time resolution, i.e., reduce asymmetry and hence increase the uncertainty, with no first order systematic effect on the early-late phase shift.

Each run at a given field is followed by a run at the same setting with an additional $4\frac{1}{2}$ feet of RG-63U cable (approximately half a cycle delay) added to the electron branch. The value of $\alpha$ should thus shift 180°. When the results are averaged, the effect of any residual asymmetry, stemming from a nonlinear phase-channel number relation, would be cancelled. No such asymmetry was in fact observed.

As a further check on the system, $\alpha_{\text{delayed}}$-$\alpha_{\text{undelayed}}$ is determined for each pair of corresponding groups in successive runs, and averaged over all runs. The mean value of this quantity is 175.5°±2.5°. This corresponds to the $4\frac{1}{2}$ feet of cable providing a delay of 5.6 nanoseconds, or a velocity of propagation of 0.80, as compared with the manufacturer's value of 0.83, times that of light in free space.

### C. Geometry

An average value for all runs of $\alpha_{\text{back}}$-$\alpha_{\text{front}}$ is also determined. The mean value is 197°±2°. This quantity is consistent with the geometric angle, $\theta_{\text{back}}$-$\theta_{\text{front}}$, between the lines of center of the forward and backward counters, as measured during the experiment, and allowing for variations in counter sensitivity with position of the event in the crystal. The results of this experiment are in no way dependent on the exact alignment of the counters, since measurements made at any angle $\theta$ should give the same early-late phase shift.

Figure 5 shows the pulse-height analyzer display for a pair of 30-minute runs at the same field setting with $4\frac{1}{2}$ feet of cable added to the electron branch in the upper run. The 180° phase shifts from front to back and from delayed to undelayed for corresponding groups are quite obvious [each display is ideally, allowing for statistical fluctuations, of the form $[1+a\cos(\phi-\alpha)]$. The early-late phase shift is about 30° in this case. It is evident that the Fourier analysis used in Eq. (13) is absolutely essential to the derivation of meaningful results.

### D. Beat Frequency Reversal

As a further check on the uniformity of the logic network (for example, leakage of the condenser in a preferred direction might cause a nonuniformity), the frequencies of the two pulsed oscillators are changed during the experiment from 1 Mc/sec below to 1 Mc/sec above that of the reference oscillator. All quantities determined by parameters occurring before this point in the apparatus (such as $\theta$, $\alpha$, $R$) remain the same, but now $\phi_\mu-\phi_e$ is displayed on the PHA, i.e., the display appears "backwards." All quantities calculated by the same formulas will thus appear to have changed sign, viz., $\alpha_{\text{early}}$-$\alpha_{\text{late}}$, $\alpha_{\text{back}}$-$\alpha_{\text{front}}$, and $\alpha_{\text{delayed}}$-$\alpha_{\text{undelayed}}$. Such is in fact observed. The resonance point is calculated separately in the two cases of pulsed oscillator frequency, and the average taken. The two agree with each other to within the stated error.

### E. Asymmetry Coefficient

Figure 6 is a graph of the coefficient, $A$, of the cosine term in $(1+A\cos\phi)$ vs magnetic field for some of the runs. The solid curve is $a/R$, as given by Eqs. (3) and (5), for $a=\frac{1}{3}$. The effect observed appears to be consistent with large values of $a$. This graph, based on $8\frac{1}{2}$

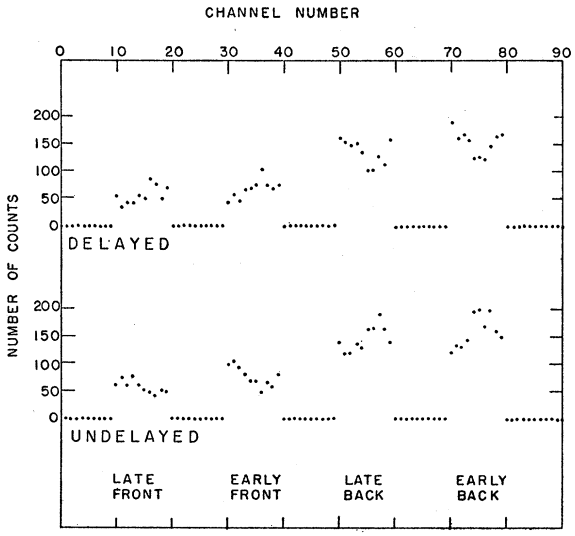


FIG. 5. Distributions, $N_\phi$, obtained in two successive half-hour runs with bromoform target. Each is ideally of the form $[1+a\cos(\phi-\alpha)]$. The upper run was taken with an additional delay of one-half cycle added to the electron pulse. The 180° phase shift between the two runs, and also between front and back of corresponding groups of the same run, is obvious. The phase shift between adjacent early and late groups is ~30° for this field setting.

hours of running, shows how difficult it would be to trace a resonance curve using the asymmetry coefficient alone. This large asymmetry is inconsistent with the broad line found by the Chicago group. Any line broadening must reduce the $a$ value for late electrons.

Effects that might decrease the asymmetry are: folding factors from finite time and geometric resolution —which could not in this experiment account for more than 15% decrease; accidental background—which was measured both by putting a long initial delay before opening the 5.7 $\mu$sec gate, and by comparing the number of early and late counts with the known gate lengths—is not more than 10% of the total counts; pions or unpolarized muons stopping in the target—which cannot be very great, because of the large observed asymmetries. These effects reduce the amplitude of the cosine term (relative to the constant average) and, therefore, reduce the accuracy of determining $\alpha$, but do not affect the magnitude of the early-late phase shift.

There remains the possibility of a residual asymmetry, if the electronics tends to favor some channels over others (e.g., a nonlinearity of the ramp might cause such an effect). This is largely cancelled by averaging delayed and undelayed runs. As a check, the counts from corresponding channels of all four groups and all the runs were added together; and the asymmetry computed is $a=0.02\pm0.02$, negligible if not zero. Since the distributions are shifted by 180° between delayed and undelayed asymmetries, the true asymmetry (due to the mu decay) should cancel leaving only the equipment asymmetry.

Periodic checks are made of the addressing circuits to insure that counts are not stored in the wrong group of channels. No wrong counts were ever observed during the run.

### F. Early-Late Time Division

The length of the multivibrator used to discriminate between early and late electrons is checked by using a variable-delay artificial pulser (double-pulser) in place of the $12\bar{3}4$ and $45\bar{1}3$ (or $23\bar{1}4$) coincidence, respectively.

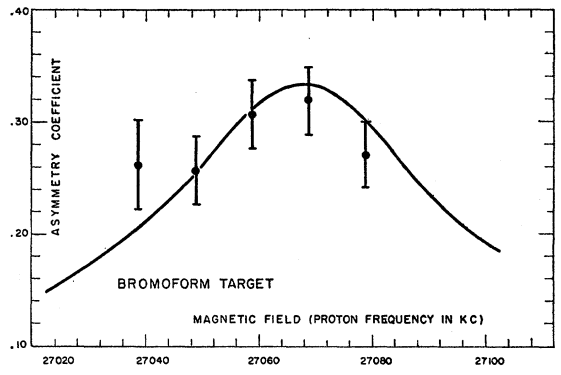


FIG. 6. Asymmetry coefficient as a function of field setting. The solid curve is given by $a/R=\frac{1}{3}[1+(\omega_H-\omega_0)^2\tau^2]^{-\frac{1}{2}}$.

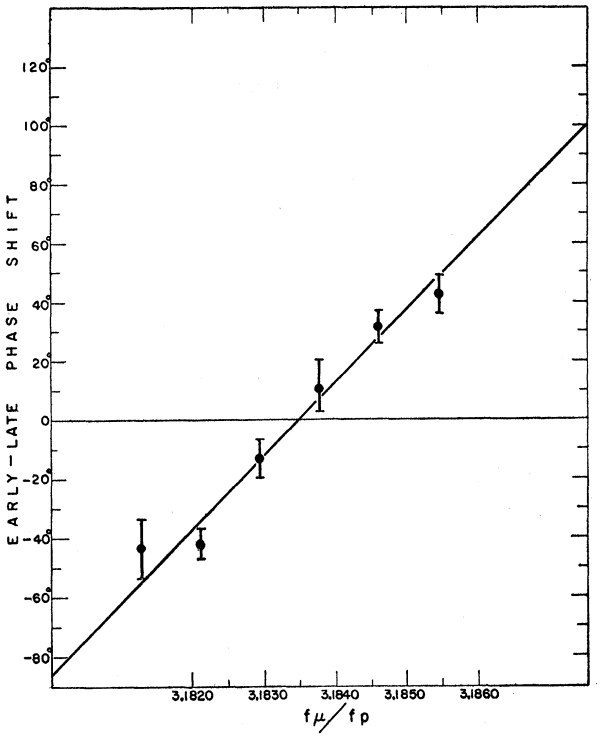


FIG. 7. ($\alpha_{\text{early}}$-$\alpha_{\text{late}}$) *vs* magnetic field (expressed as the ratio of reference frequency to proton NMR frequency). "Resonance" is determined by the intercept, which is obtained by least-square best fit of a straight line.

The delay is varied until the storage address changes from early group to late group. This separation is then measured with the calibrated sweep of an oscilloscope (nonlinearity less than 5%). For the runs used in the analysis, it is found that the length of the early gate was $1.75\pm0.05$ $\mu$sec, stable to this accuracy throughout the experiment. The late electrons fall in the remainder of the 5.7 $\mu$sec gate. For constant total gate length ($T_1+T_2$), Eq. (12) is not sensitive to variations in the division between the two. Moreover, since it is the intercept corresponding to zero phase shift between early and late as a function of magnetic field that is sought, it is not necessary to know this time to great precision.

In the analysis of the data, it is noted that in the region used, Eq. (12) does not differ appreciably from a straight line. Therefore, a least square fit to a straight line (of unknown slope and intercept) is calculated. The slope is then compared to the average slope of Eq. (12) and found to agree within the errors. Figure 7 shows the points obtained with one setting of the pulsed oscillator frequencies. The curve with the other setting is similar, having the same intercept (within the stated error) but opposite slope. The straight line is the least square best fit. The error due to statistics can be calculated from the goodness-of-fit, and agrees with that obtained using Eq. (14).

## VI. RESULTS

The ratio $f_\mu/f_p$ is found to be $3.1834\pm0.0002$.

The mass of the muon has such great bearing on the interpretation of the results of this experiment that it was considered worthwhile to re-evaluate the lower limit on the mass, as determined by experiments with mu-mesic x-rays. Koslov, Fitch, and Rainwater[16,17] found that the x-ray emitted in the $3D_{\frac{5}{2}}$-$2P_{\frac{3}{2}}$ transition in mu-mesic phosphorus ($_{15}P^{31}$), had an energy greater than that of the $K$-absorption edge in lead. The wave number of this transition is related to the mass of the muon by

$$\tilde{\nu}=\frac{5}{36}R_\infty Z^2\frac{m_\mu}{m_e}\left(1+\frac{m_\mu}{m_A}\right)^{-1}\left[1+\frac{13}{144}(Z\alpha)^2+\sum_i\delta_i\right]. \quad (15)$$

The second term is the fine structure in the Pauli-Sommerfeld approximation. The major term among the $\delta_i$ is the correction due to vacuum polarization. This can be calculated on the basis of a point nucleus using Schrödinger wave functions.[17,18] The expectation value of the "Uehling potential"[19] has been evaluated numerically to greater precision, and it is found $\delta_{\text{V.P.}}=0.003757$. Many smaller correction terms have also been calculated explicitly, and it appears they mutually cancel each other.[20] (Certain unevaluated effects which may give larger contributions than those considered by us here, such as polarization of the nucleus by the muon, and dynamic coupling with the orbital electrons, are currently under investigation.) From the results with mu-mesic x-rays it is concluded, for $Z=15$; and $m_A=30.9843$ amu.[21]

$$\frac{m_\mu}{m_e}>\frac{1}{31.25\ (1.001163)}\frac{\tilde{\nu}\ (\text{Pb } K \text{ edge})}{R_\infty},$$

and the uncertainty in this limit is mostly in the measurement of the x-ray absorption edge. This was last measured directly in 1927[22] to an accuracy of one part in 1500. The value of the $K$-absorption edge may, however, be deduced by combining $K$-emission lines with the $L$-absorption edge associated with the upper level in the lead atom. Using tabulated values of these lines[23] and the most recent values of the conversion factors,[24] one obtains $\tilde{\nu}$ (Pb $K$ edge)$=6469.2$ rydbergs. The error to be assigned must take into account the uncertainty of this procedure, the finite width of the levels, and the experimental definition of an absorption "edge." Here we shall only assume that the error in the mass lower limit is less than, or of the order of the error in the present experiment. The result so derived is

$$m_\mu>206.78\pm0.01m_e.$$

The muon $g$ factor is derived from the equation

$$g_\mu=g_p(f_\mu/f_p)(m_\mu/m_p).$$

Using[24]

$$g_p=2(2.79275\pm0.00003),\ m_p=1836.12\pm0.02m_e$$

we obtain

$$g_\mu>2(1.00122\pm0.00008),$$

compared to the quantum electrodynamical prediction of

$$g=2(1.00116).$$

## VII. CONCLUSION

The results of this experiment make it appear that the magnetic moment of the mu meson is probably not less than that predicted by quantum electrodynamics, on the assumption that the muon is a "heavy electron." The mass limit determination is still an important problem, and it is not impossible that there remain uncalculated perturbations in the energy levels of mu-mesic phosphorus, or an error in the determination of the $K$ edge in lead. Accordingly, we are repeating the important experiment of Koslov, Fitch, and Rainwater with improved energy resolution. At the same time, we are preparing to continue the present experiment at 200 Mc/sec with similar electronics but with consequent higher accuracy; and we should be able to determine the mu magnetic moment to 0.001%.

## VIII. ACKNOWLEDGMENTS

We wish to thank Professor L. M. Lederman and Professor A. M. Sachs for their collaboration in the early stages of this experiment. We also thank Professor N. M. Kroll for fruitful discussions concerning the mass of the muon, and Dr. D. H. Tycko, his staff, and Dr. W. Baker for aid in the numerical calculations on the IBM 650.

*Note added in proof.*—Experiments which have recently been reported to us [J. Lathrop, et al. and A. Bearden et al., Phys. Rev. Letters (to be published)] indicate a mass value of $M_\mu=206.76_{-0.02}{}^{+0.03}M_e$. This yields a value of $g_\mu=2(1.00113_{-0.00012}{}^{+0.00016})$. Although the assigned errors are now slightly greater than above, it is to be noted that the new result represents a direct measurement, rather than a lower limit. The agreement

[16] S. Koslov, V. Fitch, and J. Rainwater, Phys. Rev. **95**, 291 (1954).

[17] S. Koslov, Nevis Report No. 19, Columbia, 1954 (unpublished).

[18] J. Rainwater, *Annual Reviews of Nuclear Science* (Annual Reviews, Inc., Palo Alto, 1957), Vol. 7, p. 23.

[19] E. A. Uehling, Phys. Rev. **49**, 55 (1935); R. Serber, Phys. Rev. **48**, 49 (1935).

[20] A. Petermann and Y. Yamaguchi, Phys. Rev. Letters **2**, 359 (1959).

[21] H. E. Huntley, *Nuclear Species* (Macmillan and Company, Ltd., London, 1954), p. 97.

[22] J. E. Mack and J. M. Cork, Phys. Rev. **30**, 742 (1927). But see also A. J. Bearden, Phys. Rev. Letters **4**, 240 (1960).

[23] Y. Cauchois and H. Hulubei, *Tables de Constantes Selectionnees Longueurs d'Onde des Emissions et des Discontinuites d'Absorption X* (Hermann et Cie, Paris, 1947).

[24] E. R. Cohen, K. M. Crowe, and J. W. DuMond, *Fundamental Constants of Physics* (Interscience Publishers, New York, 1957).

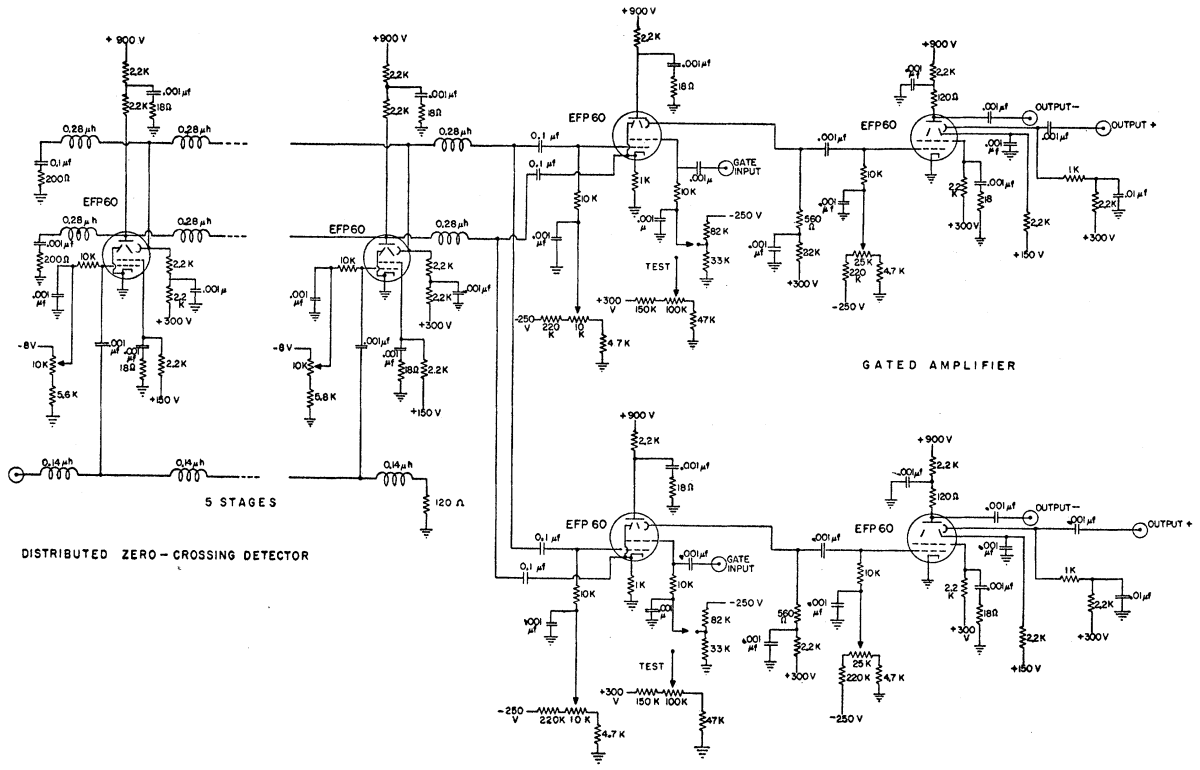


FIG. 8. Circuit diagram of zero-crossing detector.

with quantum electrodynamical theory is now quite good.

## ELECTRONIC APPENDIX

### Distributed Zero-Crossing Detector and Gated Amplifier

For the accurate timing required in this experiment, it is necessary to trigger the pulsed oscillators at times reproducible with respect to our timing criterion (the positive-going zero-crossing of the overclipped negative output of the fast counter). This means that the detection threshold should be minimal, and the output pulse rise rate be maximal. To achieve adequate sensitivity and maintain rise time, the initial stages of the zero-crossing detector are distributed. EFP-60's are employed, as shown in Fig. 8 set just above the edge of conduction (conducting about 1 ma). The circuit output commences when the positive swing of the overclipped counter pulse had reached 5% of its maximum value or about 0.5 volt.

The final two stages are separated into two branches, gated, respectively, by the $\mu$ and $e$ outputs of the gating circuit. Switches are provided so that they may be operated ungated for test purposes. The trigger circuits actuated by the zero-crossing circuit output have time delays which are a function of the input pulse size and rise time. To minimize the timing uncertainty, the output pulses of the zero-crossing circuit are produced by driving the output EFP 60 well into saturation and clipping the output. The pulse thus obtained is large (30 volts into 60Ω) and constant in amplitude. The overall timing uncertainty obtained is less than $5\times10^{-10}$ sec.

### Pulsed Oscillators

A circuit diagram of the pulsed oscillators is shown in Fig. 9. A trigger circuit, ($V_1$, $V_2$), like those described in the gating circuit, is used to turn on a Hartly-type oscillator for 6 $\mu$sec by applying a fast-rising 200-v pulse to the screen of the 6AK5, ($V_3$). Screen to control grid capacitance injects enough of the proper Fourier component into the tank circuit to obtain reliable starting. To reduce starting transients in the output of the circuit, which would disturb the low-frequency amplifiers, the final stage is a 6AS6 amplifier ($V_4$) normally biased off at the suppressor and turned on slowly with the oscillator gate through a low pass RC time constant $\sim$0.5 $\mu$sec. By the time the 6AS6 has attained full gain, starting transients in the oscillator have disappeared.

As a test of starting phase stability, the two pulsed oscillators adjusted to nearly the same frequency were triggered simultaneously with the zero-crossing outputs and beat together. A shift of $5\times10^{-10}$ sec in starting time could have been easily detected by eye on the oscilloscope screen and was not observed. This result is

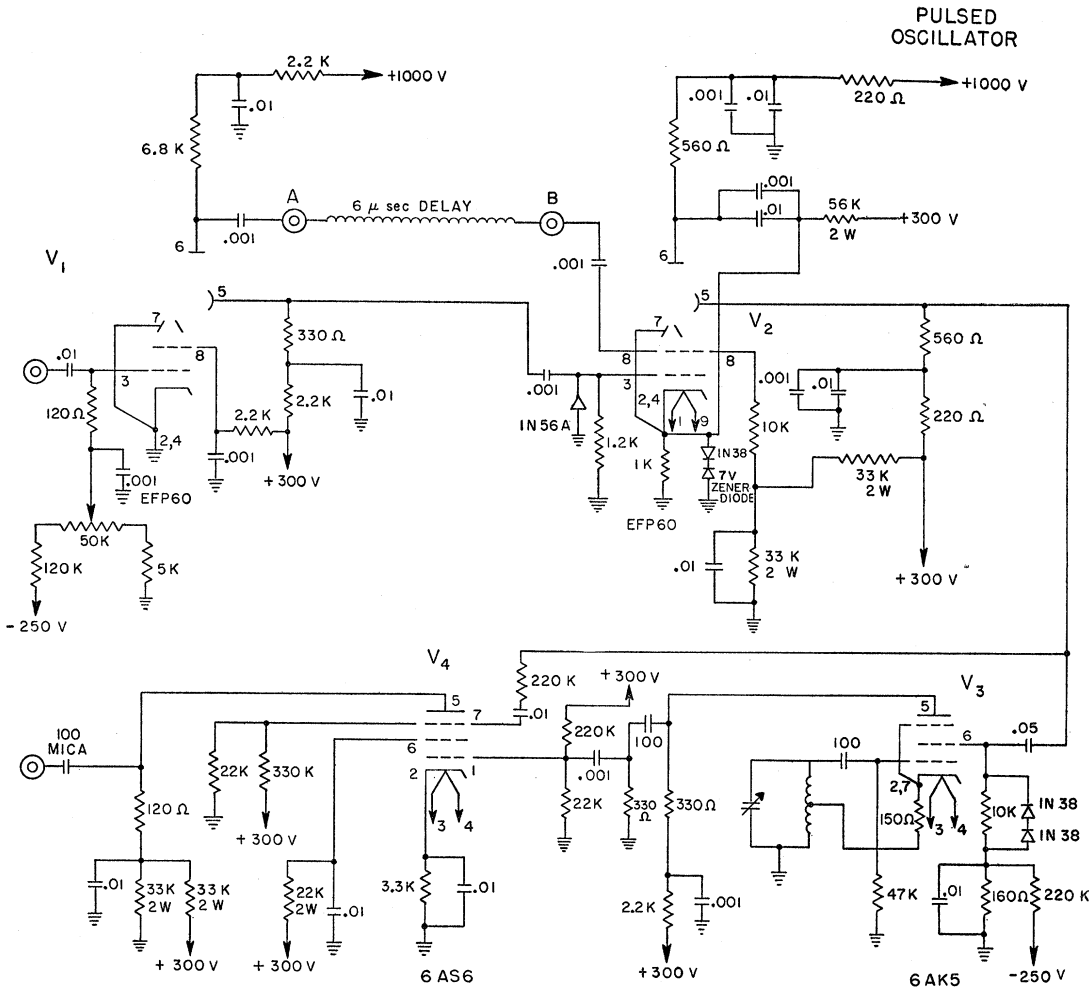


FIG. 9. Circuit diagram of pulsed oscillator.

confirmed by the over-all system check described elsewhere in this paper.

## Logic Network

The reference oscillator voltage is of the form $e^{i(\omega_0 t+\phi)}$, where $\phi$ is the phase at $t=0$, i.e., when the event being measured occurs. After transients have disappeared, the pulsed oscillator voltage is of the form $Ae^{i[(\omega_0-\beta)t+\gamma]}$ where $A$ is the relative amplitude of the signal, $\beta$ the difference frequency, which was chosen to be 1 Mc/sec, $\gamma$ the fixed arbitrary starting phase of the pulsed oscillator. The combined signal is then $e^{i(\omega_0 t+\phi)}[1+Ae^{-i(\beta t+\phi-\gamma)}]$. If a condenser is charged at a constant rate from $t=0$ until $\beta t+\phi-\gamma=(\pi/2)+2\pi n$ where $n$ is the number of cycles ignored so that transients disappear, the charge stored will be linear in $\phi$. If one charges this condenser for a time corresponding to $\phi_\mu$, and discharges it for a time corresponding to $\phi_e$, the charge remaining will be linear in $\phi\equiv\phi_e-\phi_\mu$, the quantity of interest in this experiment.

The block diagram of the logic network which yields a pulse whose amplitude is proportional to $\phi$ is shown in Fig. 10. The combined signal is rectified and filtered. The envelope is converted into a square wave by the clipping amplifier using stabistor diodes with a stable forward conducting threshold of 0.2 v. The square wave is differentiated so that a train of alternating positive and negative short pulses at half-microsecond intervals is obtained.

The relation between $\phi$ and the clipped pulse time will be linear only after the clipping amplifier has recovered from starting transients. Therefore, an "enable" multivibrator is introduced which opens a gate one microsecond after the ramp start. A coincidence is made in the "gated multivibrator," with the first subsequent positive pulse of the train. This is an improvement over the circuit of Chase and Higinbotham,[14] in which an unavoidable nonlinearity distorted a considerable portion of the cycle. In the present circuit, one waits for a cycle or more of the beat frequency until all effects of

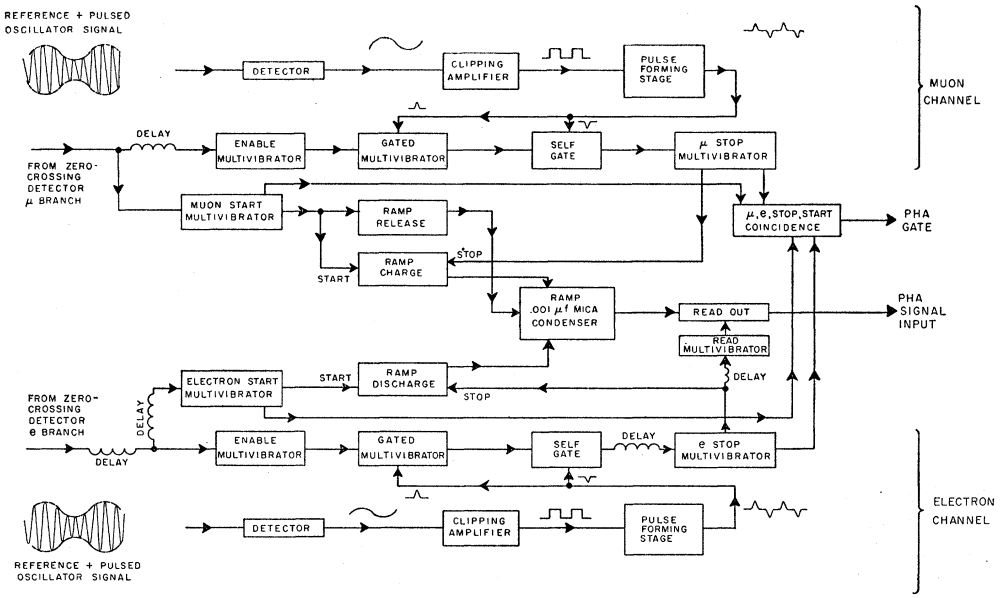


FIG. 10. Block diagram of logic network.

the finite pass-band of the amplifier on the sudden start of the beat note have died away.

The problem arises of the distortion of pulses falling during the rise of the "enable" gate. The ramp is, therefore, stopped not with the first positive pulse after the enable pulse but with the next following negative pulse after the first positive pulse. The "self-gate" is primed by the output of the gated multivibrator, and it then passes the next negative pulse from the train 0.5 $\mu$sec later which triggers the stop multivibrator. The combined time jitter of the start and stop multivibrator is less than $\pm 0.05$ $\mu$sec. Worse jitter than this would worsen the time resolution, but has no first order effect on the measurement.

The negative output of the zero-crossing amplifier is used to trigger the start multivibrator. A fourfold coincidence between "start" and "stop" outputs from both $\mu$ and electron channels is required before any signal will be stored in the PHA. Switches are provided to eliminate this requirement from either side for test purposes.

The ramp condenser that stores the charge proportional to $\phi_\mu - \phi_e$ is initially clamped to ground with two vacuum diodes. These diodes are cut off with the muon start multivibrator output and remain so until after the readout.

The ramp charge pulse allows the ramp to be charged through a vacuum diode and two paralleled 100K deposited carbon precision ($\pm 1\%$) resistors, by cutting off the tube which holds the diode plate below ground. The ramp will charge until the ramp charge stop pulse pulls the diode plate below ground. The "stop" output always outlasts the "start." Similarly, the ramp discharge circuit allows the ramp to discharge through two 100K precision resistors and a diode. The ramp circuit is thus made independent of tube characteristics since charging rates are determined by fixed resistors in series with vacuum diodes whose voltage drop in the forward direction is negligible compared with that across the charging resistors. The use of vacuum diodes throughout minimizes leakage currents stemming from finite back resistances. Leakage of the ramp condenser, which could introduce a systematic error, was checked and found to be negligible. The discharging rate may be varied with a potentiometer, in series with the fixed resistors. This will compensate for the frequencies of the pulsed oscillators not being identical. Adjustment is made for best time resolution as indicated by viewing the PHA when the same input is fed to both $\mu$ and $e$ channels.

The read multivibrator is triggered by the electron "stop" pulse after a delay to make sure all charging and discharging is complete. The read-out gated cathode follower gives an output linear in the charge on the ramp condenser with an adjustable pedestal.